Full-Metal Six-Port Switched-Beam Antenna Based on Capacitively Loaded Monopoles in an Annular Cavity for S-Band NTN/HAPS

Javier Vera-Sánchez, Miguel Ferrando-Rocher, Gorka Casasus-Goyeneche, Miguel Ferrando-Bataller
Antennas and Propagation Lab, iTEAM Research Institute, Universitat Politècnica de València (UPV), Spain
jversan2@upv.es

***Abstract*—This paper presents an all-metal, six-port switched-beam antenna concept aimed at S-band Non-Terrestrial Networks (NTN) and High-Altitude Platform Stations (HAPS). The radiator set consists of six capacitively loaded monopoles (top-hat posts) embedded in a shallow annular cavity. Internal metallic septa are used to condition the cavity fields and to bias the radiation toward mid-elevation angles, which is desirable for HAPS-to-ground coverage. By exciting one port at a time while terminating the remaining ports, the antenna generates six directive beams providing full azimuthal coverage through electronic switching. Full-wave simulations confirm strong impedance matching over 2.5 GHz to 4.0 GHz and coupling levels consistent with practical switched-beam operation. The fully metallic implementation avoids dielectric materials, improving robustness against harsh environmental conditions.**

***Index Terms*—All-metal antenna, S-band, NTN, HAPS, switched-beam, multi-port antenna, annular cavity, capacitively loaded monopole.**

I. Introduction

Non-terrestrial network layers are moving from "nice-to-have" demonstrations into engineering-driven architectures where coverage, capacity, and interference management must be treated jointly. For mobile NTN in particular, antenna technology is increasingly discussed together with distributed array concepts and coordinated precoding strategies that can reshape spatial selectivity at the system level [1], [2]. In parallel, integrated terrestrial–satellite terminals are pushing compact multi-band and shared-aperture front-ends, where S-band is often a practical anchor due to propagation robustness and sub-6 GHz implementation maturity [3], [4].

Within the NTN ecosystem, High-Altitude Platform Stations (HAPS) have emerged as a complementary layer positioned between terrestrial infrastructure and satellite systems, enabling regional coverage with reduced latency and flexible deployment. Several advanced concepts have been proposed to enhance HAPS communications performance, including the integration of Reconfigurable Intelligent Surfaces (RIS) to passively steer signals and improve energy efficiency [5], [6]. However, such approaches typically introduce increased system complexity, higher power requirements, and reliance on active components or dielectric materials that may be vulnerable to the harsh stratospheric environment, potentially affecting long-term reliability.

From the HAPS standpoint, the antenna payload's job is to radiate power to illuminate the service region with as little waste as possible. A purely zenith-directed beam is rarely optimal unless the service is strictly nadir-centric. The typical scenario involves a wide-area footprint with useful links at mid-elevation angles. In many deployments, the payload also benefits from a beam set that can be selected dynamically without requiring a full multi-channel phased array. That middle ground between a single fixed beam and a true phased array is precisely where switched-beam architectures remain attractive.

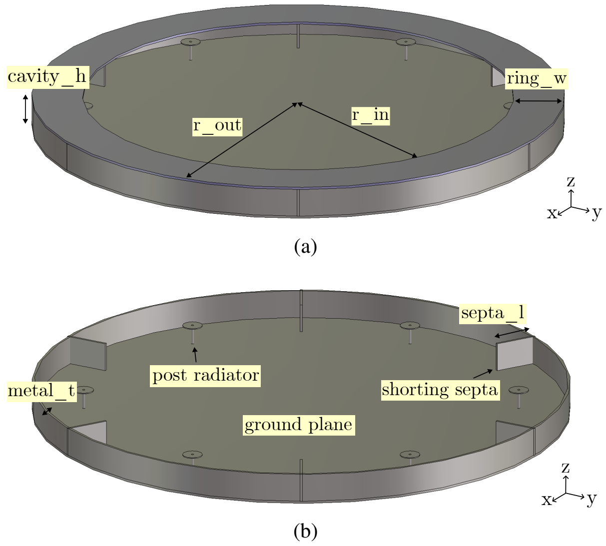

Fig. 1. All-metal annular-cavity switched-beam antenna concept. The six ports are placed azimuthally; internal septa are used to condition the cavity fields and promote mid-elevation radiation.

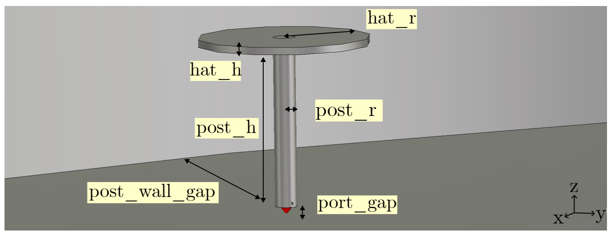

Fig. 2. Detail view of one radiating element: a capacitively loaded monopole implemented as a metallic post terminated by a circular top-hat disk. The surrounding cavity and septa contribute additional reactive loading and beam shaping.

This work proposes a mechanically robust all-metal antenna capable of generating six azimuthal sectors though beam-switching using a single structure with six feed ports. Cavity-backed switched-beam antennas have proven well suited for mechanically robust surveillance payloads, with Space ADS-B implementations demonstrating this approach at L-band [7], [8]. In this paper, that architectural principle is re-optimized and scaled to S-band, targeting NTN/HAPS terminals where a single RF chain plus an RF switching network provides a practical compromise between spatial selectivity, hardware complexity, and reliability. The remainder of this paper is organized as follows. Section II describes the antenna architecture and beam-switching concept. Section III presents simulated impedance and radiation results. Section IV concludes the paper and outlines future developments.

II. Antenna Architecture

The proposed structure is depicted in Fig. 1 and Fig. 2. The antenna comprises a solid metal ground plane and an outer annular wall that forms a shallow cavity. Six radiating elements are distributed azimuthally and excited through six independent ports. Each element is realized as a metallic post terminated by a circular disk (top-hat). A set of internal metallic septa is introduced inside the cavity region; these features alter the boundary conditions and the field distribution, which in turn biases the far-field beam away from purely vertical illumination.

The top-hat increases the effective capacitance at the radiator tip, allowing the element to reach resonance and improved matching without requiring a taller post. From a design-intuition standpoint, the radiator can be interpreted through a simple resonance picture where the post contributes an inductive component and the disk plus its environment provides an effective capacitance. In practice, the radiator does not operate in isolation: the cavity contributes reactive loading, suppresses back radiation, and stabilizes current paths. The internal septa further influence the cavity fields in a controlled manner, which is exploited here to shape the beam toward mid-elevation angles.

The operating mode is intentionally simple. One port is excited while the other five ports are terminated in 50 Ω. Under this condition, the excited radiator dominates and the cavity/septa environment shapes the resulting beam. Switching the active port rotates the main lobe in azimuth, providing a six-sector coverage solution with a single RF chain and an RF switching network. The aim is not to replace a phased array, but to provide a practical beam-set with considerably lower RF complexity while still enabling a degree of spatial selectivity consistent with NTN-oriented trends.

Full-wave electromagnetic simulations were performed in CST Studio Suite. The structure was modeled as a perfect electric conductor (PEC) in this stage. Multi-port S-parameters were computed by exciting one port at a time and matching the remaining ports. The same termination condition was used for radiation computations, so that each reported pattern corresponds to a realistic switched state.

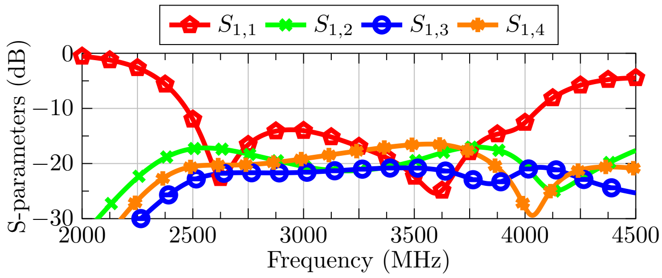

Fig. 3. Simulated S-parameters magnitude for the six-port structure under matched terminations. The antenna is well matched over the target 2.5 GHz to 4.0 GHz region, with coupling levels consistent with port-switched operation.

The performance is assessed over the full simulated band from 2 GHz to 4.5 GHz, with particular attention to the region where the design is intended to operate and the matching is strongest. Besides input matching, inter-port coupling is evaluated with the non-excited ports terminated in 50 Ω to ensure that inactive ports remain well behaved in each switched state. Radiation patterns are reported at 3 GHz, close to the band centre, where the mid-elevation beam bias introduced by the annular cavity and the internal septa is clearly observed.

III. Simulated Results

The simulated S-parameters magnitude is reported in Fig. 3. The input reflection coefficient exhibits its best behavior across 2.5 GHz to 4 GHz, where $|S_{11}|$ remains below −10 dB and typically reaches values around −25 dB to −14 dB. Outside that range the matching degrades progressively, which is consistent with a fixed-geometry top-hat radiator embedded in a cavity where higher-order reactive effects become increasingly relevant. Coupling between ports remains within levels compatible with switched-beam operation. Inactive radiators do not capture a dominant fraction of the launched power, which is important for efficiency and for maintaining pattern stability across switching states. In practical hardware, these coupling levels also ease the requirements on the switching network because excessive leakage into off-states tends to distort the effective illumination.

The switched-beam behavior is summarized in Fig. 4, which collects the simulated 3D realized-gain patterns at 3 GHz for each port state. The core observation is repeatability: as the excited port moves from Port 1 to Port 6, the main lobe rotates accordingly, producing six distinct azimuth sectors while preserving a broadly comparable lobe shape. This can be seen directly by comparing Fig. 4a through Fig. 4f.

A further observation is the nature of the beam tilt itself. Although the main lobe rotates cleanly in azimuth, its elevation angle remains broadly consistent from port to port, confirming the expected azimuthal symmetry of the structure. In an all-metal cavity-backed structure this behavior is plausible and, in fact, expected: the annular boundary and the internal septa break the “free-space monopole” symmetry and bias the cavity-supported current paths, imposing a preferential illumination angle that is identical for all six sectors. The

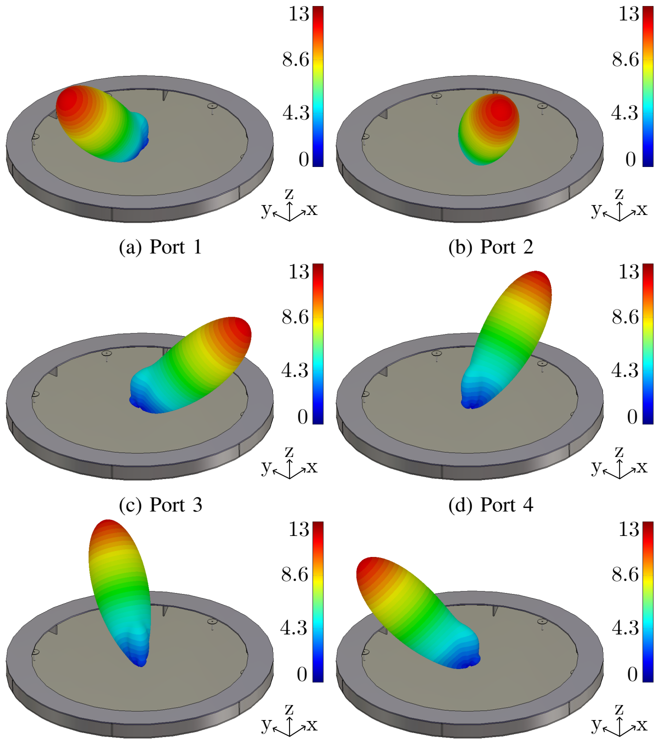

(a) Port 1 (b) Port 2 (c) Port 3 (d) Port 4 (e) Port 5 (f) Port 6

Fig. 4. Simulated 3D realized-gain patterns at 3 GHz in linear scale for the six switched states. The main beam rotates in azimuth with port selection, yielding six-sector coverage within a single-column figure.

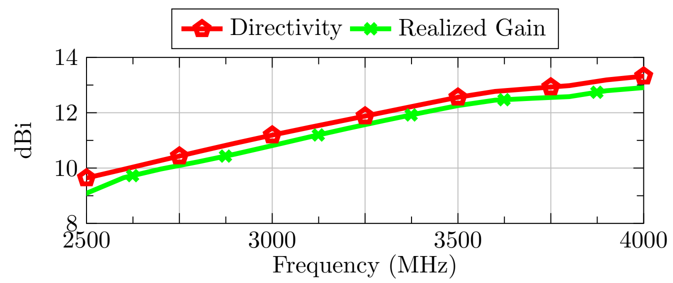

Fig. 5. Simulated realized gain and directivity.

peak realized gain is consistently around 11 dBi for each port, confirming directive sector operation with a single compact structure.

IV. Conclusion

An all-metal six-port switched-beam antenna concept for S-band NTN/HAPS has been presented. The design combines capacitively loaded monopoles with an annular cavity and internal septa, achieving strong impedance matching across 2.5 GHz to 4 GHz while delivering six directive beams that rotate with port selection. Simulations at 3 GHz show repeatable sectorized radiation with peak realized gains around 11 dBi. Ongoing work will quantify beam metrics (peak direction, beamwidth, and crossover levels) across the full band and will incorporate manufacturability tolerances and experimental validation.

TABLE I
Key geometrical parameters of the proposed antenna.

Parameter	Value	**Parameter**	Value
Outer cavity radius, r_out	115 mm	Inner cavity radius, r_in	93 mm
Cavity height, cavity_h	12.12 mm	Top ring height, ring_w	0.36 mm
Septa length, septa_l	18.66 mm	Metal thickness, metal_t	1 mm
Post height, post_h	8.32 mm	Post radius, post_r	0.55 mm
Top-hat height, hat_h	0.36 mm	Top-hat radius, hat_r	4.28 mm
Feeding port gap, port_gap	0.36 mm	Post gap, post_wall_gap	21 mm

TABLE II
Simulated total radiation efficiency

f (GHz)	Directivity (dBi)	Realized Gain (dBi)	η_{tot}
2.5	9.6	9.1	0.88
3.0	11.2	10.8	0.91
3.5	12.6	12.3	0.93
4.0	13.3	12.9	0.91

Acknowledgment

This research was conducted within the SATERA project, which has received funding from the SESAR 3 Joint Undertaking (JU) under grant agreement No. 101164313, with support from the European Union's Horizon Europe research and innovation programme and the SESAR 3 JU members other than the Union. Additional support was provided by Spain's Ministerio de Ciencia e Innovación under research projects PID2022-136869NB-C33 and PID2022-141055NB-C21.

References

[1] G. Bacci, R. de Gaudenzi, M. Luise, L. Sanguinetti, and E. Sebastiani, "Formation-of-arrays antenna technology for high-throughput mobile nonterrestrial networks," *IEEE Transactions on Aerospace and Electronic Systems*, vol. 59, no. 5, pp. 4919 – 4935, 2023.

[2] R. de Gaudenzi, G. Bacci, M. Luise, L. Sanguinetti, and P. Angeletti, "Applicability of CF-MIMO Precoding to a Formation of Arrays (FoA) for Mobile Satellite Communications," *IEEE Transactions on Aerospace and Electronic Systems*, vol. 61, no. 5, pp. 11 069 – 11 087, 2025.

[3] J. Wu, Y. Cheng, Y. Wang, C. Liao, and X. Ding, "S-/k-/ka-band shared-aperture antenna with polarization diversity for system integration of terrestrial and satellite mobile communications," *IEEE Antennas and Wireless Propagation Letters*, vol. 24, no. 11, pp. 4097 – 4101, 2025.

[4] F. Tiezzi, C. Domínguez, J. Padilla, N. Ortiz, M. C. Viganò, and S. Vaccaro, "User terminal antennas for s-band mobile satellite communication systems," *International Journal of Satellite Communications and Networking*, vol. 32, no. 4, pp. 277 – 289, 2014.

[5] K. An, Y. Sun, Z. Lin, Y. Zhu, W. Ni, N. Al-Dhahir, K.-K. Wong, and D. Niyato, "Exploiting multi-layer refracting ris-assisted receiver for hap-swipt networks," *IEEE Transactions on Wireless Communications*, vol. 23, no. 10, pp. 12 638–12 657, 2024.

[6] N. Gao, S. Jin, X. Li, and M. Matthaiou, "Aerial RIS-Assisted High Altitude Platform Communications," *IEEE Wireless Communications Letters*, vol. 10, no. 10, pp. 2096–2100, 2021.

[7] J. Vera-Sánchez, M. Ferrando-Rocher, G. Casasus-Goyeneche, and M. Ferrando-Bataller, "L-Band Unit-Cell Antenna Design for Satellite-Based ADS-B Surveillance," in *2025 IEEE International Symposium on Antennas and Propagation and North American Radio Science Meeting (AP-S/CNC-USNC-URSI)*, 2025, pp. 1893–1895.

[8] J. Vera-Sánchez, A. Martín-Núnez, M. Ferrando-Rocher, and M. Ferrando-Bataller, "Circularly Polarized Conical Array for ADS-B Applications in LEO Satellites," in *2025 19th European Conference on Antennas and Propagation (EuCAP)*, 2025, pp. 1–3.